ANDREW MATAS

KAGRA TELECON, JUNE 1, 2018

SEARCHES FOR THE STOCHASTIC GRAVITATIONAL WAVE BACKGROUND IN ADVANCED LIGO'S FIRST OBSERVING RUN

STOCHASTIC GRAVITATIONAL WAVE BACKGROUND

A superposition of astrophysical and cosmological sources, including…

Unresolved astrophysical sources (binaries, supernovae, NS, …)

Superradiance, axion clouds …

Early Universe
(inflation, pre big-bang, …)

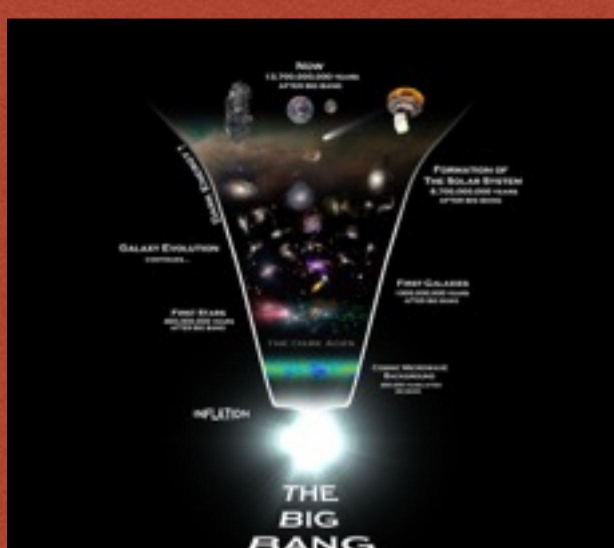

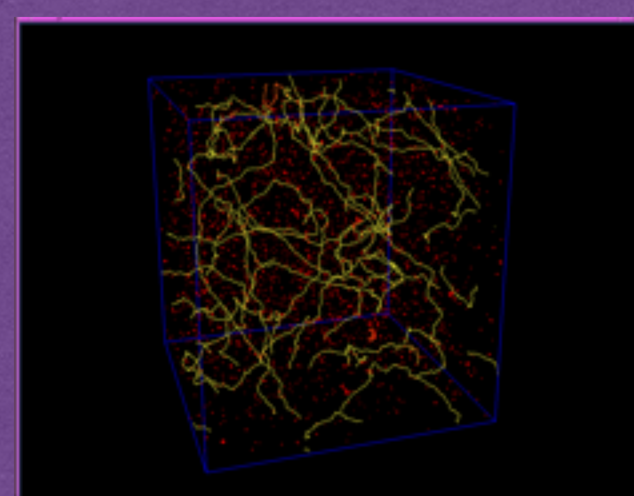

Cosmic Strings

Cosmological
Phase Transitions

CHARACTERIZING THE STOCHASTIC BACKGROUND

'Stochastic waveforms' are random time series, need to characterize the background statistically

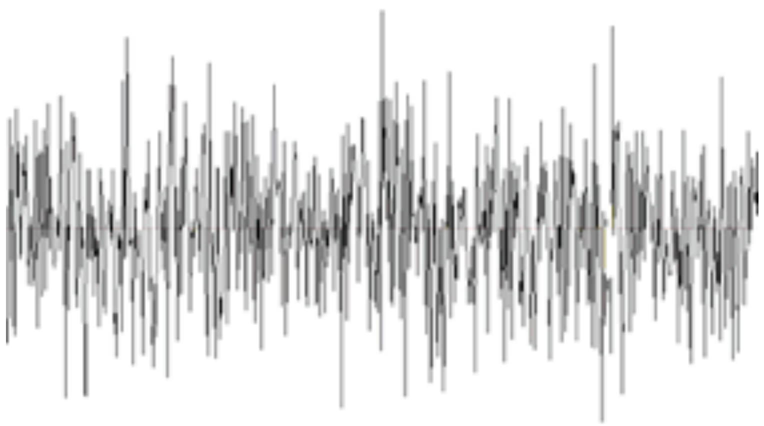

Assuming background is statistically:

Gaussian

isotropic

unpolarized

stationary

it is fully characterized by energy density

$$\Omega_{\rm GW}(f) = \frac{1}{\rho_c}\frac{d\rho_{\rm GW}}{d\log f}$$

$$\rho_{\rm GW} = \frac{c^2}{32\pi G}\langle \dot{h}_{ab}(t,\vec{x})\dot{h}^{ab}(t,\vec{x})\rangle$$

Allen and Romano, Phys.Rev. D59 (1999) 102001

DATA ANALYSIS TECHNIQUE

Cross correlate the time series from 2+ detectors

The signal is long duration and non-deterministic

$$s_1 = h_1 + n_1$$
$$s_2 = h_2 + n_2$$

signal and noise are uncorrelated

$$\langle s_1 s_2 \rangle = \boxed{\langle h_1 h_2 \rangle} + \langle h_2 n_1 \rangle + \langle h_1 n_2 \rangle + \langle n_1 n_2 \rangle$$

signal

noise at 2 widely separated detectors is uncorrelated

Allen and Romano, Phys.Rev. D59 (1999) 102001

OVERLAP REDUCTION FUNCTION

Cross correlation of detector outputs is related to $\Omega_{\rm GW}$

$$\langle \tilde{s}_1(f)^\star \tilde{s}_2(f) \rangle = \frac{3H_0^2}{20\pi^2}\delta(f-f')|f|^{-3}\Omega_{\rm GW}(|f|)\gamma(|f|)$$

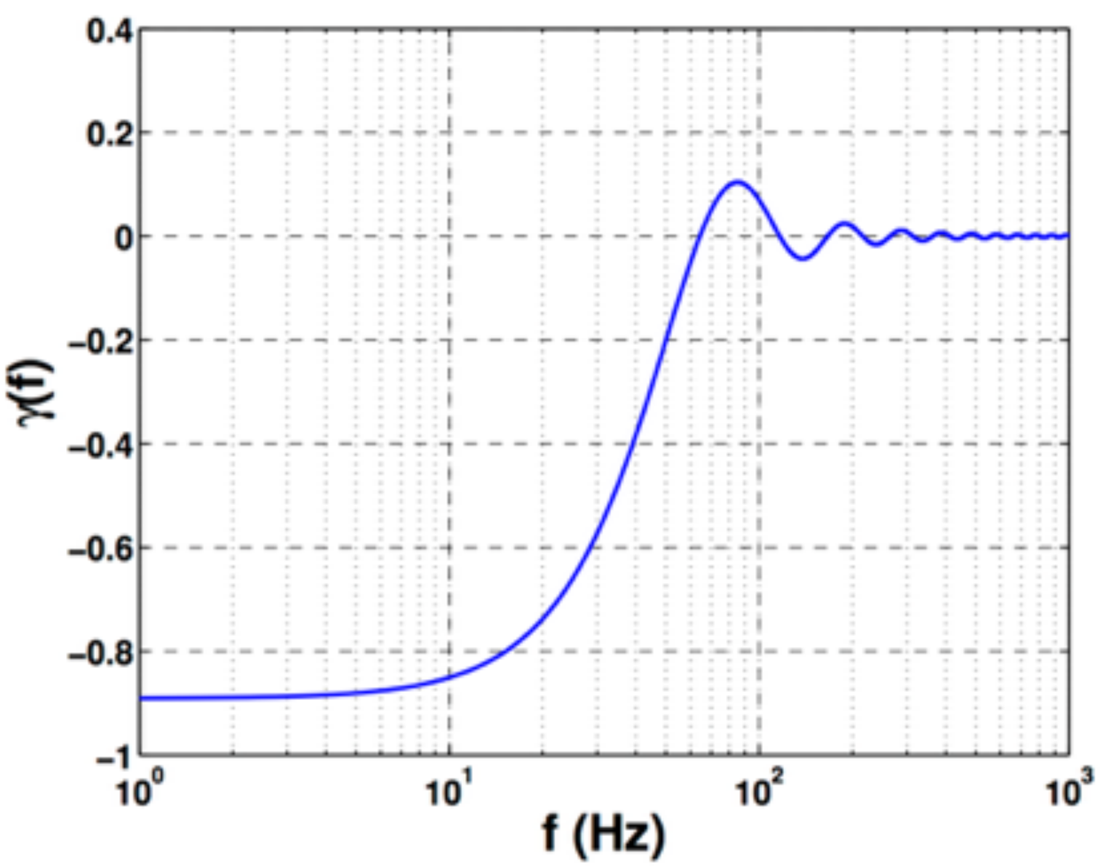

Allen and Romano, Phys.Rev. D59 (1999) 102001

Overlap reduction function

time delay

$$\gamma(f) := \frac{5}{8\pi}\sum_A \int_{S^2} d\hat{\Omega}\, e^{i2\pi f \hat{\Omega}\cdot\Delta\vec{x}/c} F_1^A(\hat{\Omega}) F_2^A(\hat{\Omega})$$

detector response

Geometric factor controlling sensitivity

OPTIMAL FILTER

Allen and Romano, Phys.Rev. D59 (1999) 102001

Cross correlate detectors with filter function Q

$$Y = \int_{-\infty}^{\infty} \mathrm{d}f\, \tilde{s}_1^\star(f)\tilde{s}_2(f)\tilde{Q}(f)$$

Choose filter function to maximize SNR (assuming noise >> signal)

$$\tilde{Q}(f) = \lambda \frac{\gamma(f)\Omega(f)H_0^2}{f^3 P_1(f) P_2(f)}$$

λ is chosen so $\langle Y \rangle = \Omega_{\mathrm{GW}}$

Uncertainty (assuming ideal case that detector noise is stationary and Gaussian)

$$\sigma^2 \approx \frac{T}{4} \int_{-\infty}^{\infty} \mathrm{d}f\, P_1(|f|)P_2(|f|)|\tilde{Q}(f)|^2$$

SNR scales like sqrt(T)

$$\mathrm{SNR} := \frac{\mu}{\sigma} \approx \frac{3H_0^2}{10\pi^2} \sqrt{T} \frac{\int_{-\infty}^{\infty} df\ |f|^{-3}\ \Omega_{\mathrm{gw}}(|f|)}{\left[\int_{-\infty}^{\infty} df\ P_1(|f|)P_2(|f|)\right]^{1/2}}$$

COMBINING RESULTS FROM MULTIPLE DETECTORS

Allen and Romano, Phys.Rev. D59 (1999) 102001

Combine results from each detector pair Y_{IJ}

I,J label detectors used in the cross-correlation procedure described on previous slides

Optimal combination of cross-correlation statistic from *N* detectors:

$$Y_{\text{network}} = \sum_{I=1}^{N} \sum_{J=1}^{I-1} Y_{IJ} \qquad \sigma_{\text{network}}^{-2} = \sum_{I=1}^{N} \sum_{J=1}^{I-1} \sigma_{IJ}^{-2}$$

Scaling with number of detectors in network, assuming similar sensitivity and co-located detectors

$$\sigma_{\text{Network}} \sim N_{\text{pairs}}^{-1/2} \sim N^{-1}$$

In practice, this scaling breaks down due both to the fact that different detectors have different noise curves, and due to network geometry (different overlap reduction functions)

OVERLAP REDUCTION FUNCTION FOR {H,L,V,K} PAIRS

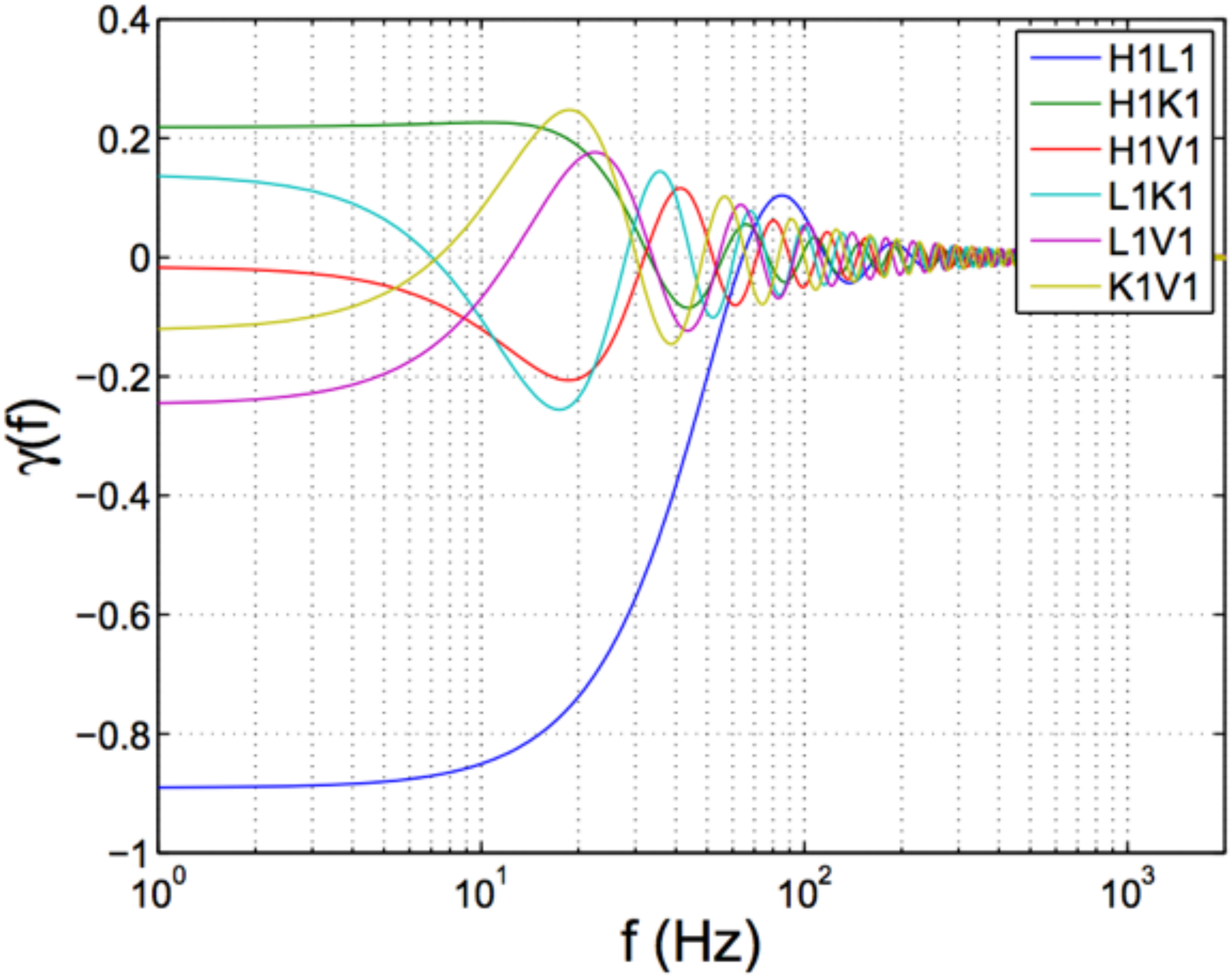

Thrane and Romano, Phys.Rev. D88 (2013) no.12, 124032

EFFECT OF NETWORK GEOMETRY ON SENSITIVITY

Assume a network of detectors with positions and orientations of H1,L1,V1,K1, with aLIGO design sensitivity noise curves

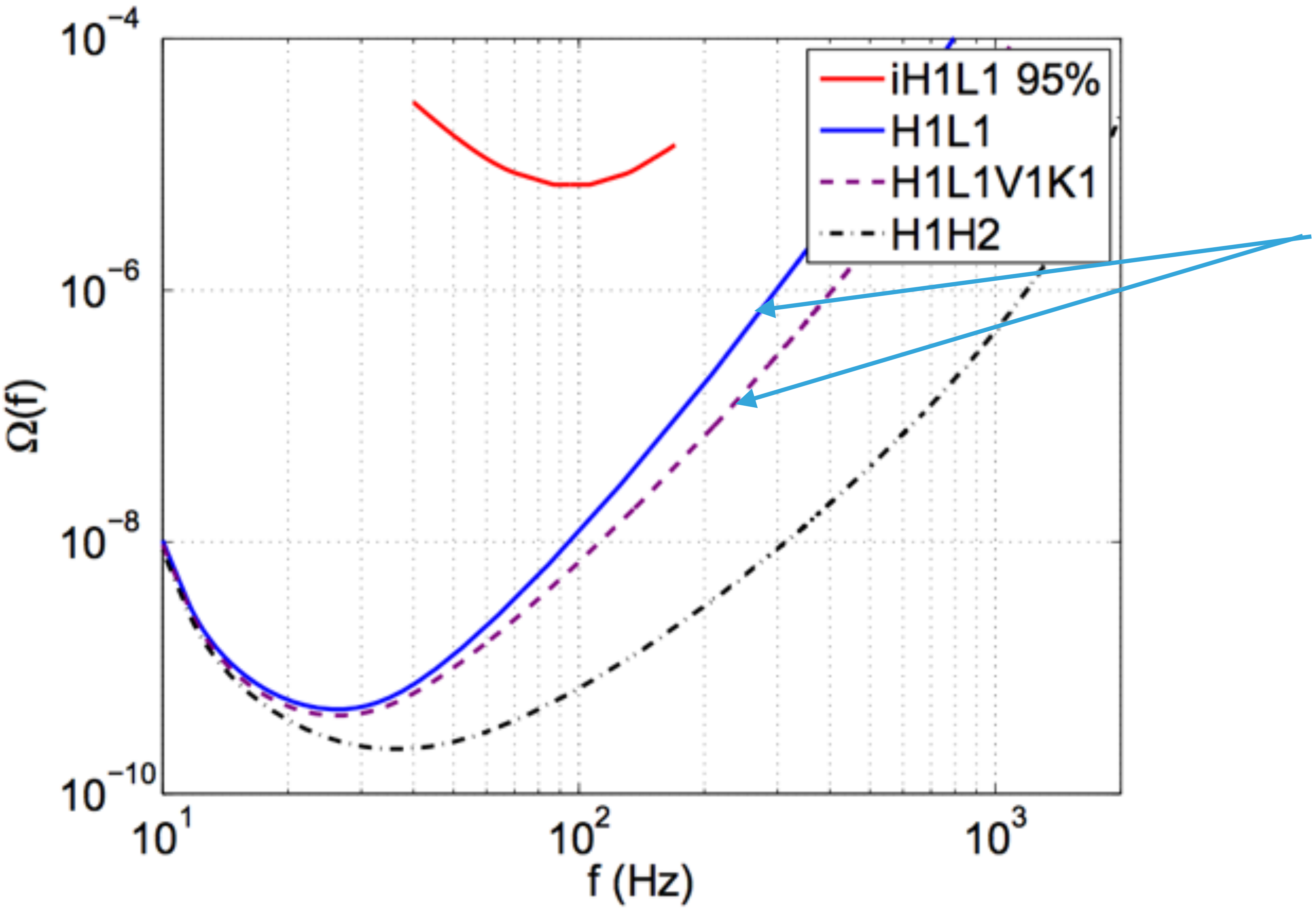

Improvement largest at high frequencies (power laws with a large positive spectral index)

Thrane and Romano, Phys.Rev. D88 (2013) no.12, 124032

ANALYSIS OF LIGO'S FIRST OBSERVING RUN

We analyzed data at H1 and L1 from first observing run (O1) September 2015–January 2016

Hanford, Washington (H1)

Livingston, Louisiana (L1)

Image credit: LIGO Lab

ANALYSIS CUTS

1. We remove times where data is known to be corrupt (for example: interferometer not operational)

2. We remove time segments where noise is non-stationary

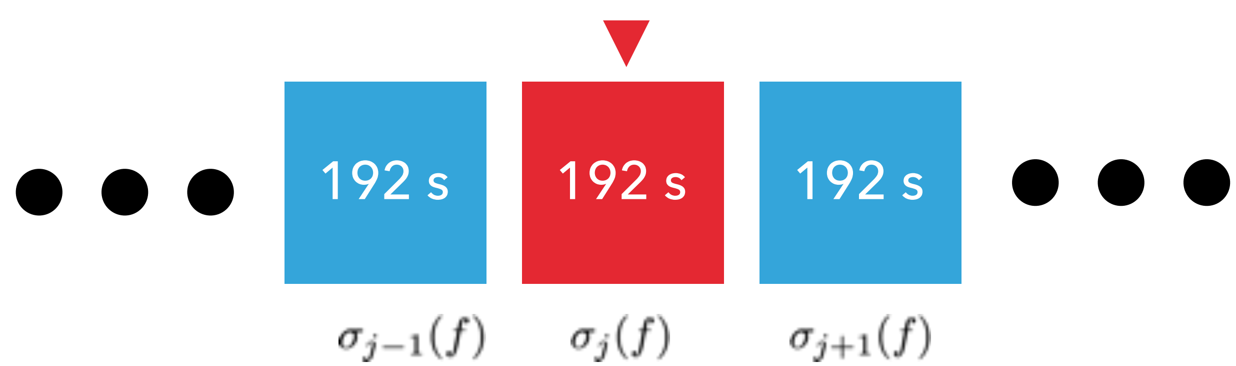

$$\left|\sigma_j - \frac{\sigma_{j+1} + \sigma_{j-1}}{2}\right| \leq 0.2\sigma_j$$

3. We remove frequency bins which display coherence with instrumental (auxiliary) channels

Abbott *et al*, Phys.Rev.Lett. 118 (2017) no.12, 121101

RESULTS

Upper limits for specific (fixed) values of α

Spectral index α	Frequency band with 99% sensitivity	Amplitude Ω_α	95% CL upper limit	Previous limits [33]
0	20 – 85.8 Hz	$(4.4 \pm 5.9) \times 10^{-8}$	1.7×10^{-7}	5.6×10^{-6}
2/3	20 – 98.2 Hz	$(3.5 \pm 4.4) \times 10^{-8}$	1.3×10^{-7}	–
3	20 – 305 Hz	$(3.7 \pm 6.5) \times 10^{-9}$	1.7×10^{-8}	7.6×10^{-8}

$$\Omega_{\rm GW}(f) = \Omega_\alpha \left(\frac{f}{f_{\rm ref}}\right)^\alpha$$

Upper limit improves by a factor of **33** over Initial LIGO for alpha=0, due to the large increase in sensitivity of Advanced LIGO

$\alpha = 0$ Inflation, cosmic strings in our band…

$\alpha = 2/3$ Binary inspiral (BBH, BHNS, BNS)

Abbott et al, Phys.Rev.Lett. 118 (2017) no.12, 121101

COMPARING MODELS AND OTHER BOUNDS

Abbott et al, Phys.Rev.Lett. 118 (2017) no.12, 121101

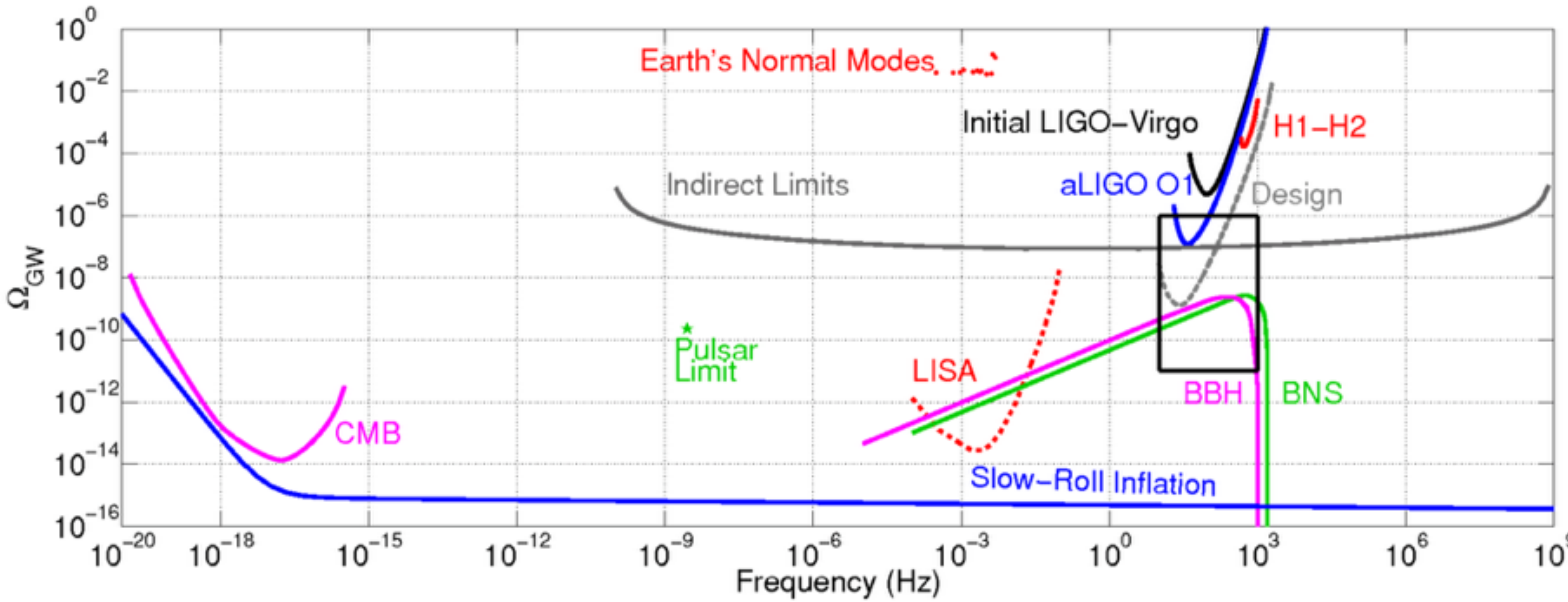

Black box will be discussed in more detail in a few slides

2 sigma sensitivity curves are shown using power law integrated form

Indirect limits combine CMB and Big Bang Nucleosynthesis measurements

LISA projection described in Thrane and Romano 2013

Abbott et al, Phys.Rev.Lett. 118 (2017) no.12, 121101

COMPACT BINARY BACKGROUND

Superposition of many BBH, BNS, BHNS systems

Astrophysical foreground for cosmological models

Contains information about astrophysics

binary formation rate

energy spectrum for single binary

$$\Omega_{\mathrm{GW}}(f,\theta_k) = \frac{f}{\rho_c H_0}\int_0^{z_{\max}} \mathrm{d}z \frac{R_m(z,\theta_k)\frac{\mathrm{d}E_{\mathrm{GW}}(\theta_k)}{\mathrm{d}f}}{(1+z)E(\Omega_M,\Omega_\Lambda,z)}$$

cosmology

$$\Omega_{\mathrm{GW}}(f) = \int \mathrm{d}\theta_k P(\theta_k)\Omega_{\mathrm{GW}}(f,\theta_k)$$

Source parameters $\theta_k = \{m_1, m_2, \chi\}$

Abbott et al, Phys.Rev.Lett. 118 (2017) no.12, 121101

REDSHIFT DEPENDENCE

$R_m(z)$ assumed to follow star formation rate with time delay to account for difference between formation and merger

Most sources at 1<z<3

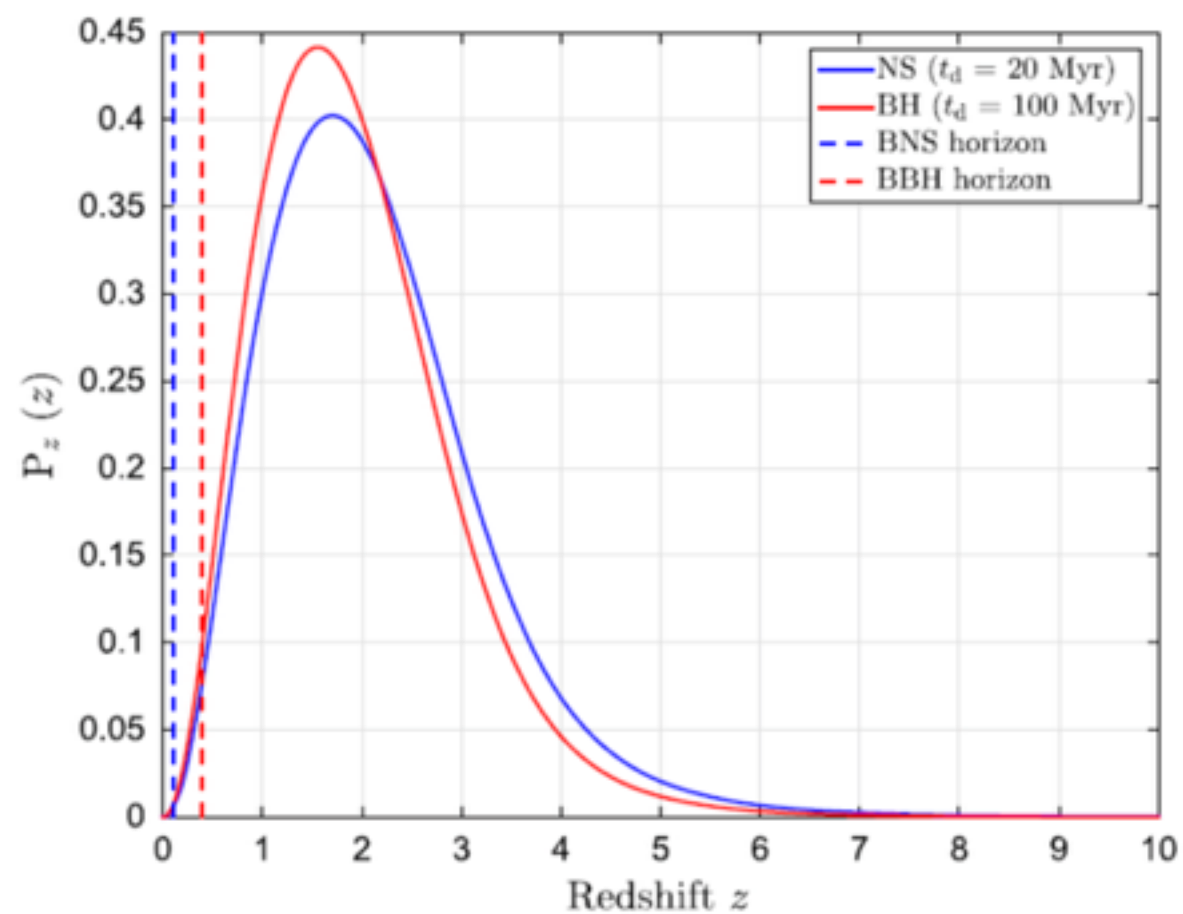

Meacher et al Phys.Rev.D 92, 063002 (2015)

SPECTRUM

Median total spectrum is roughly a factor of 1.6 larger than spectrum from BBH alone

Expect to dig into interesting parameter space in O3

Significant upgrades planned between O2 and O3, especially at low frequencies

	$\Omega_{GW}(25\text{ Hz})$
BNS	$0.7^{+1.5}_{-0.6} \times 10^{-9}$
BBH	$1.1^{+1.2}_{-0.7} \times 10^{-9}$
Total	$1.8^{+2.7}_{-1.3} \times 10^{-9}$

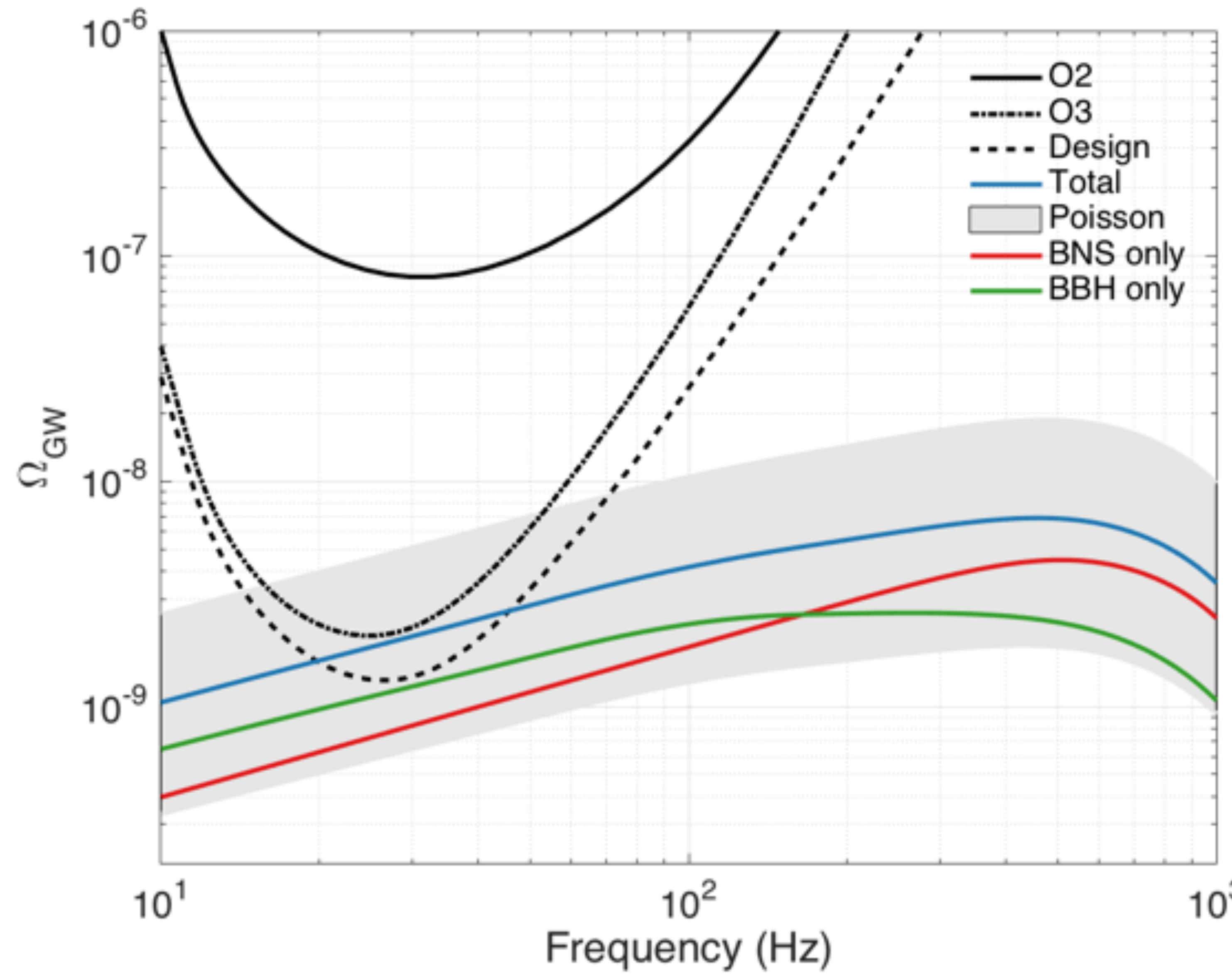

Abbott et al, 1710.05837

DETECTABILITY

With median rates, expect to see signal with SNR=3 after 40 months of observation time (a few months into Design sensitivity)

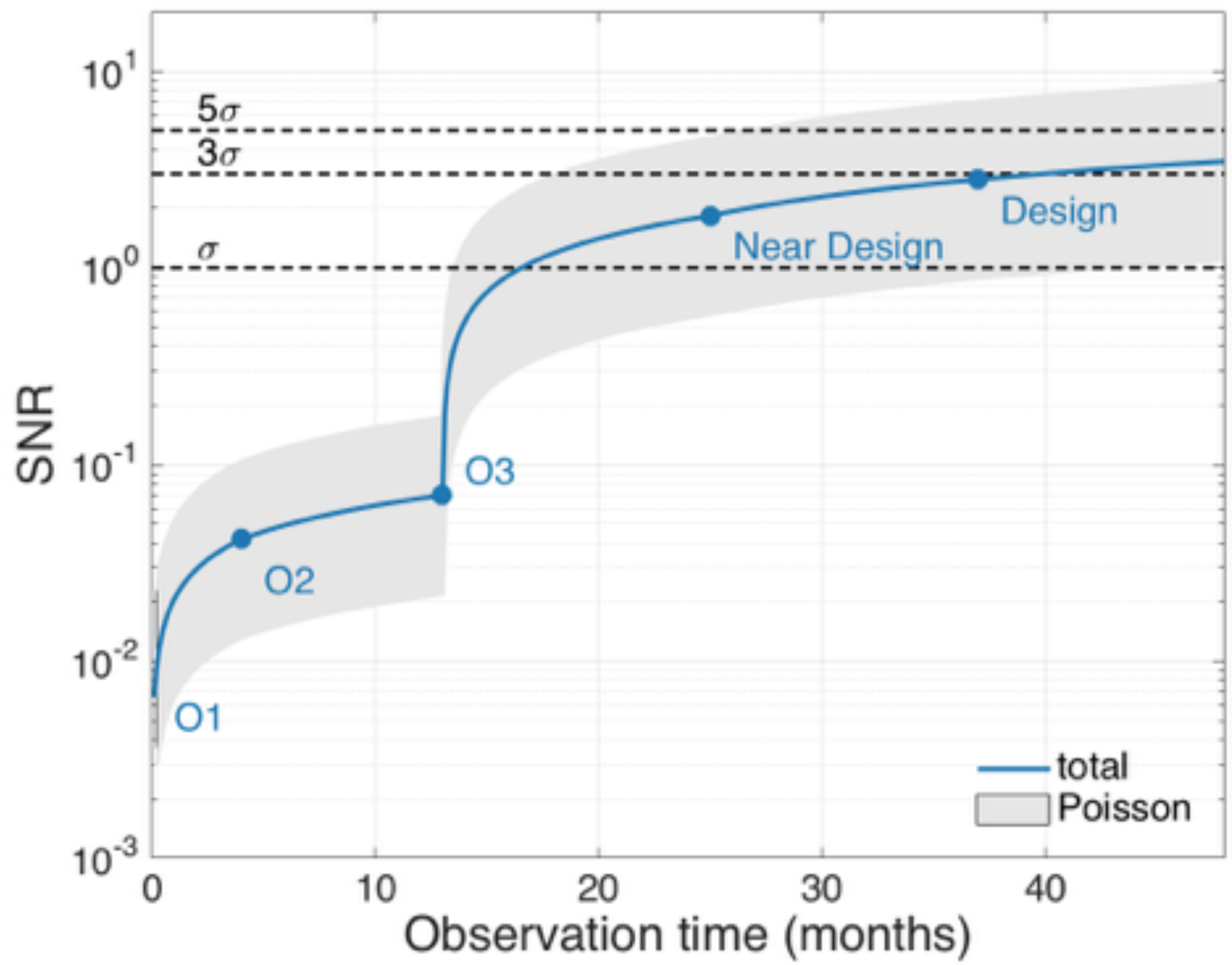

Abbott et al, 1710.05837

"POPCORN" VS CONTINUOUS

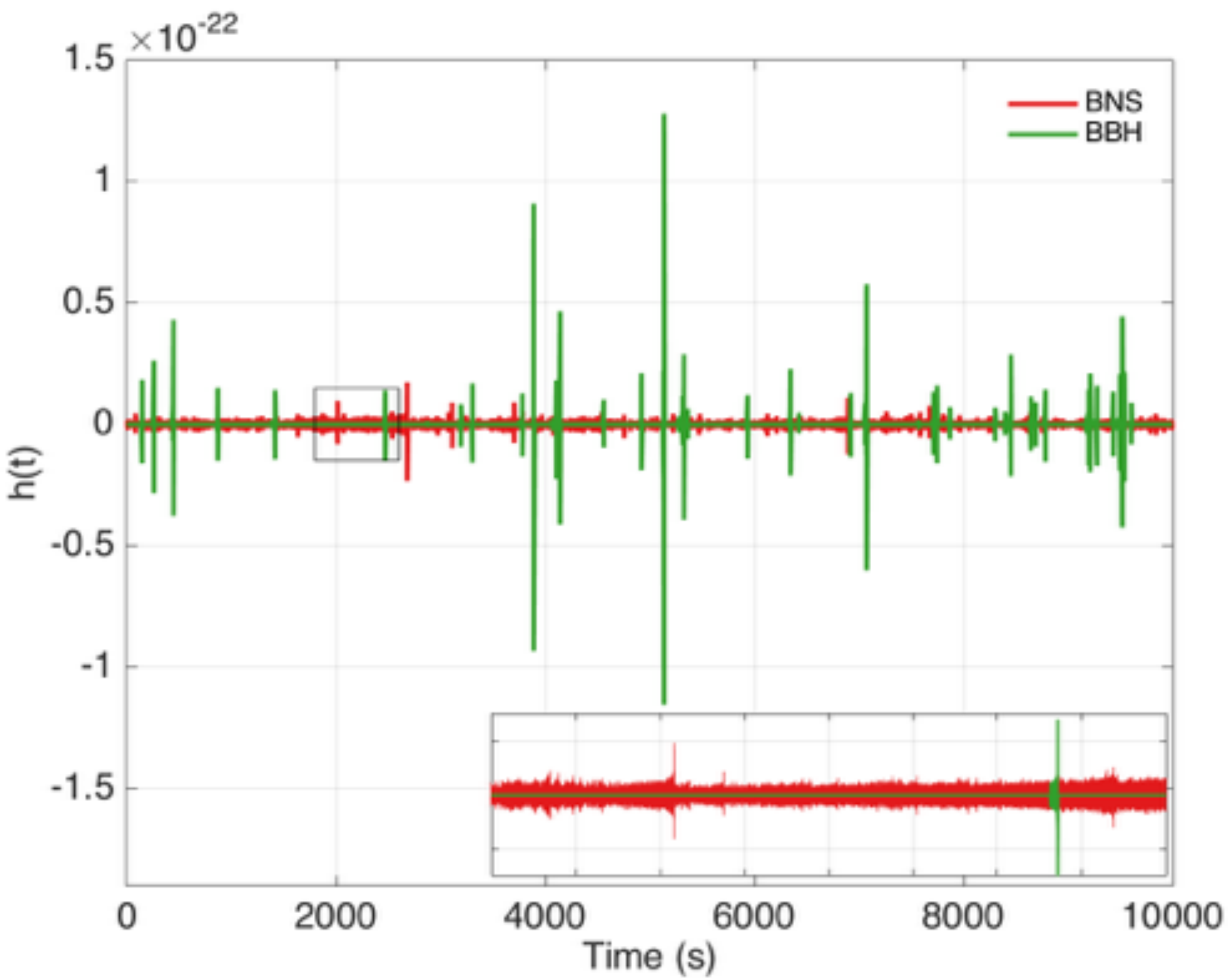

BNS signals overlap in time domain

BBH signals are short and do not overlap

Abbott et al, 1710.05837

UNIVERSITY OF MINNESOTA

ANISOTROPIC BACKGROUND

$$\langle h_A^*(f,\hat{\Omega}) h_{A'}(f',\hat{\Omega}')\rangle = \frac{1}{4}\mathcal{P}(f,\hat{\Omega})\delta(f-f')\delta_{AA'}\delta(\hat{\Omega},\hat{\Omega}')$$

Typically assume $\mathcal{P}(f,\hat{\Omega}) = \mathcal{P}(\hat{\Omega})\bar{H}(f)$

Expand $\mathcal{P}(\Theta)$ in a basis

$$\mathcal{P}(\Theta) = \mathcal{P}_\alpha \mathbf{e}_\alpha(\Theta)$$

$\mathbf{e}_\alpha(\Theta) = \delta^2(\Theta, \Theta_\alpha)$

Radiometer search

point sources

$\mathbf{e}_\alpha(\Theta) = Y_{\ell m}(\Theta)$

Spherical harmonic search

Abbott *et al*, Phys.Rev.Lett. 118 (2017) no.12, 121102

SPHERICAL HARMONIC: BROADBAND, ALL SKY SEARCH

All-sky (broadband) Results

						Max SNR (% p-value)		Upper limit range	
α	Ω_{gw}	$H(f)$	f_α (Hz)	θ (deg)	l_{max}	BBR	SHD	BBR ($\times 10^{-8}$)	SHD ($\times 10^{-8}$)
0	constant	$\propto f^{-3}$	52.50	55	3	3.32 (7)	2.69 (18)	10 – 56	2.5 – 7.6
2/3	$\propto f^{2/3}$	$\propto f^{-7/3}$	65.75	44	4	3.31 (12)	3.06 (11)	5.1 – 33	2.0 – 5.9
3	$\propto f^{3}$	constant	256.50	11	16	3.43 (47)	3.86 (11)	0.1 – 0.9	0.4 – 2.8

SNR

90% UL

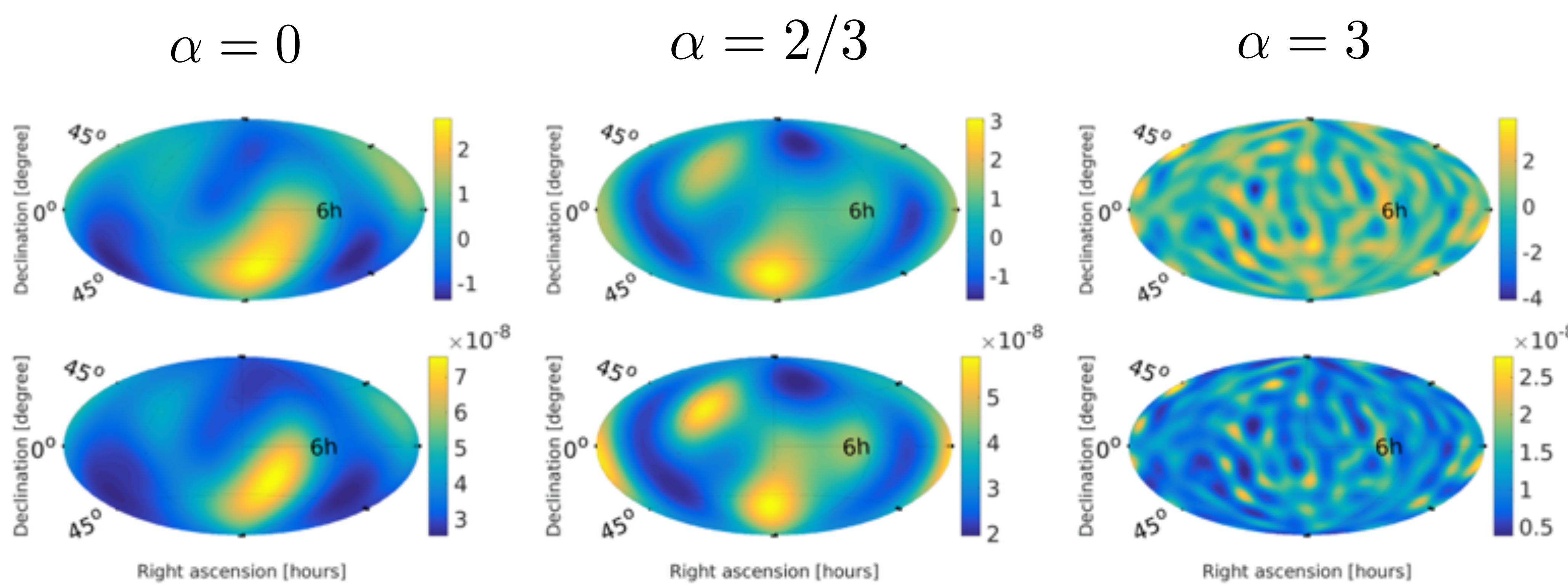

Abbott *et al*, Phys.Rev.Lett. 118 (2017) no.12, 121102

About a factor of 60 improvement over Initial LIGO for alpha=0

UPPER LIMITS ON CL

Alternative representation used by CMB experiments

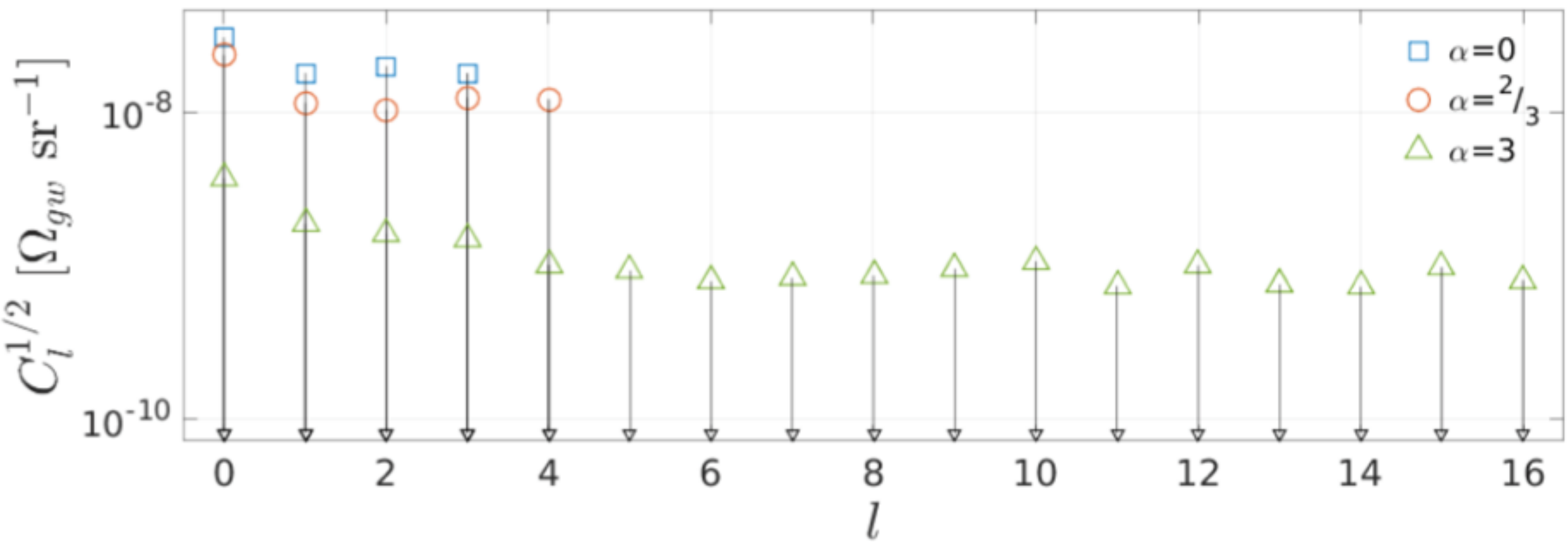

Abbott *et al,* Phys.Rev.Lett. 118 (2017) no.12, 121102

$$C_l = \frac{1}{2l+1}\sum_{m=-l}^{l} |\mathcal{P}_{lm}|^2$$

University of Minnesota

RADIOMETER: BROADBAND, ALL SKY SEARCH

						All-sky (broadband) Results			
						Max SNR (% p-value)		Upper limit range	
α	Ω_{gw}	$H(f)$	f_α (Hz)	θ (deg)	l_{max}	BBR	SHD	BBR ($\times 10^{-8}$)	SHD ($\times 10^{-8}$)
0	constant	$\propto f^{-3}$	52.50	55	3	3.32 (7)	2.69 (18)	10 – 56	2.5 – 7.6
2/3	$\propto f^{2/3}$	$\propto f^{-7/3}$	65.75	44	4	3.31 (12)	3.06 (11)	5.1 – 33	2.0 – 5.9
3	$\propto f^{3}$	constant	256.50	11	16	3.43 (47)	3.86 (11)	0.1 – 0.9	0.4 – 2.8

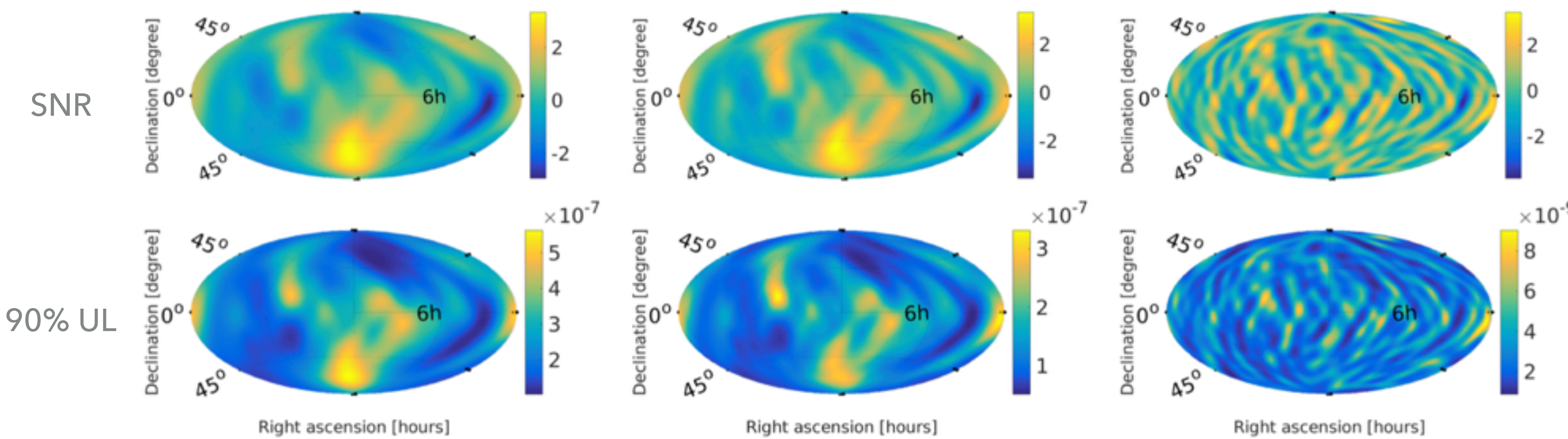

About a factor of 8 improvement in flux over Initial LIGO for $\alpha = 3$

Abbott *et al,* Phys.Rev.Lett. 118 (2017) no.12, 121102

RADIOMETER: NARROWBAND RESULTS FOR SPECIAL DIRECTIONS

Abbott *et al,* Phys.Rev.Lett. 118 (2017) no.12, 121102

Narrowband Radiometer Results

Direction	Max SNR	p-value (%)	Frequency band (Hz)	Best UL ($\times 10^{-25}$)	Frequency band (Hz)
Sco X-1	4.58	10	616 – 617	6.7	134 – 135
SN1987A	4.07	63	195 – 196	5.5	172 – 173
Galactic Center	3.92	87	1347 – 1348	7.0	172 – 173

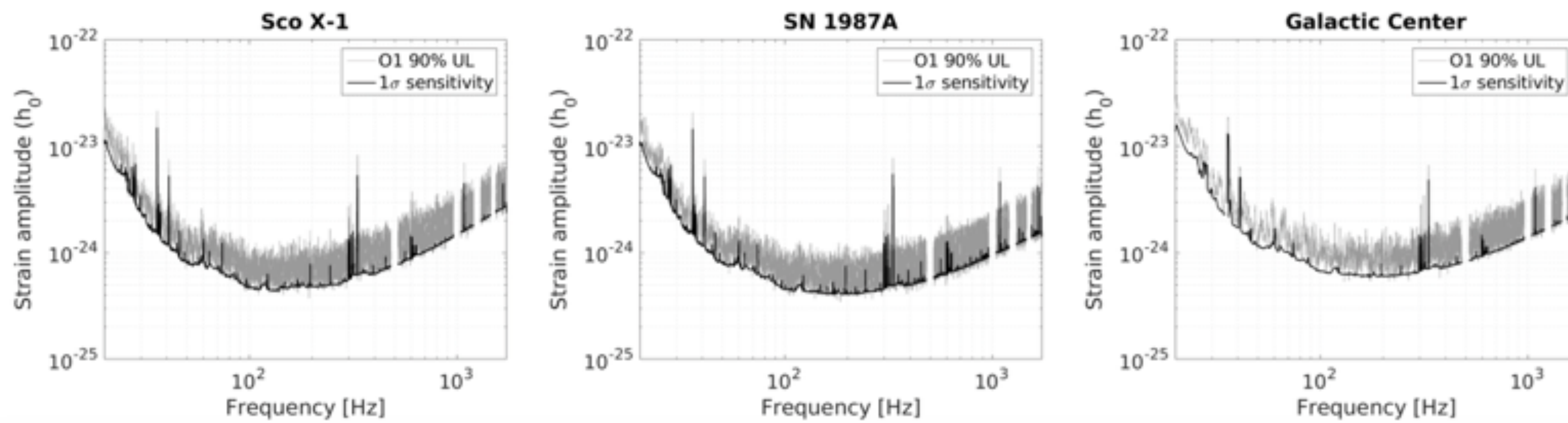

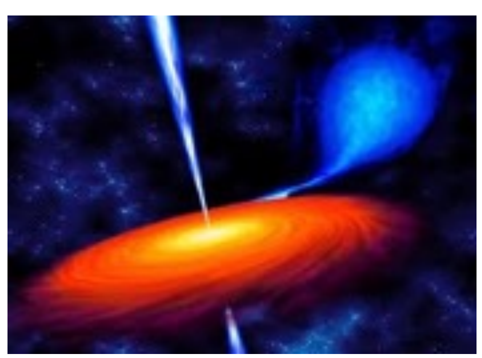

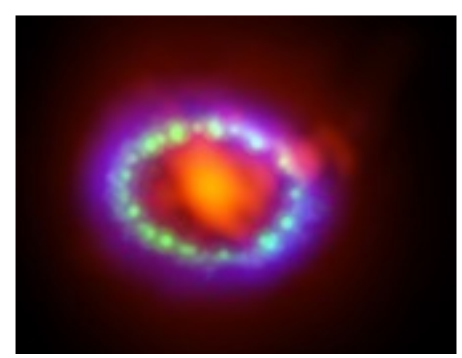

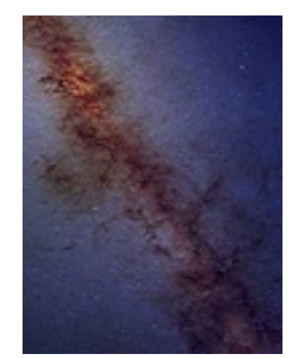

Improves over Initial LIGO results by about a factor of 10 below 50 Hz and above 300 Hz and by about a factor of 2 on average across the band

ANGULAR RESOLUTION

Angular resolution limited by:
* Diffraction limit
* Blind directions –> **a larger detector network reduces need to handle blind directions**

$$\hat{\mathcal{P}}'_{\alpha} = (\Gamma'^{-1})_{\alpha\beta}\, X_{\beta}$$

Clean Map
What we want
(GW power
in every sky direction)

Inverse Fisher matrix / beam pattern matrix

- Not truly invertible due to blind directions
- Typically this is regularized by SVN
- **A detector network naturally regulates this matrix**

Dirty Map
Result of cross
correlation

Thrane et al, Phys.Rev. D80 (2009) 122002

REGULARIZATION OF FISHER MATRIX

More detectors => Reduced error on each component of map => Better recovery on all angular scales

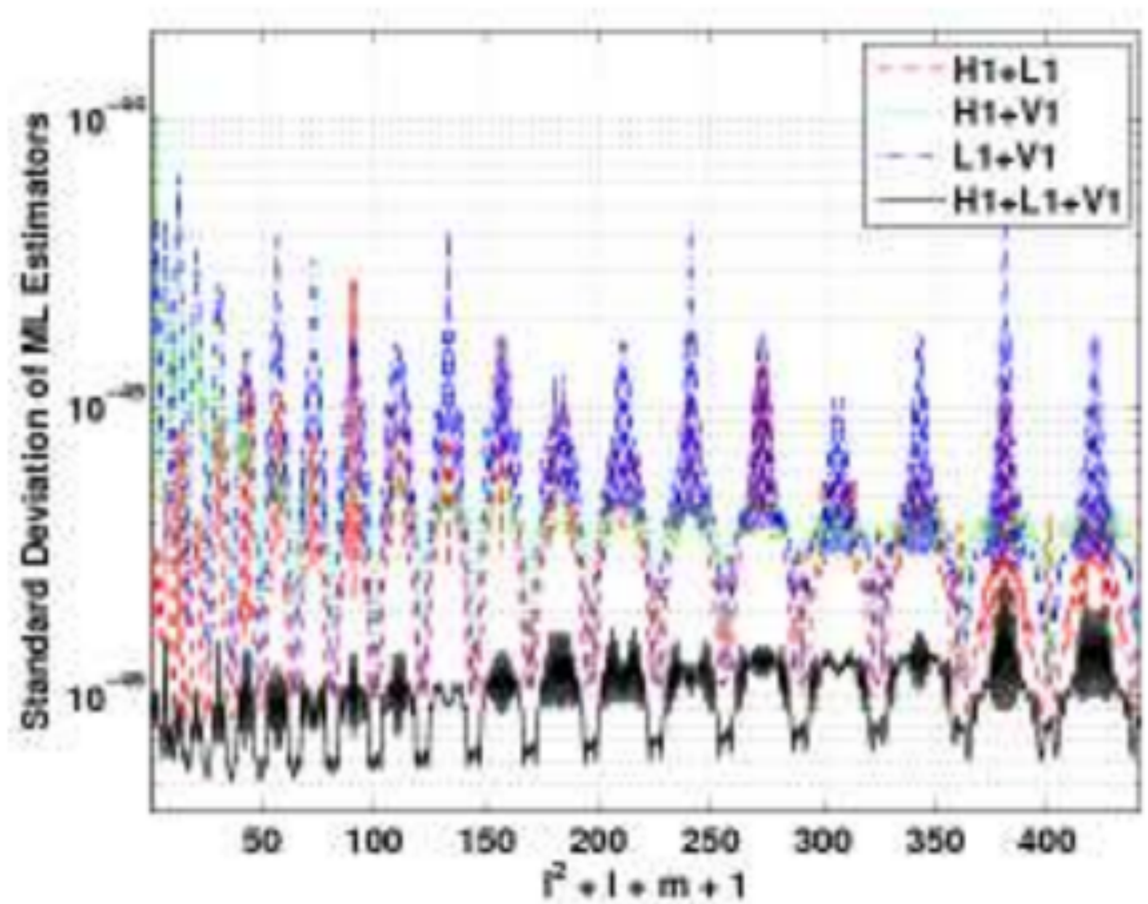

This plot is phrased in terms of spherical harmonics, but a similar result applies to radiometer

Thrane et al, Phys.Rev. D80 (2009) 122002

NON-TENSOR POLARIZATIONS

6 polarizations for a symmetric 3x3 tensor

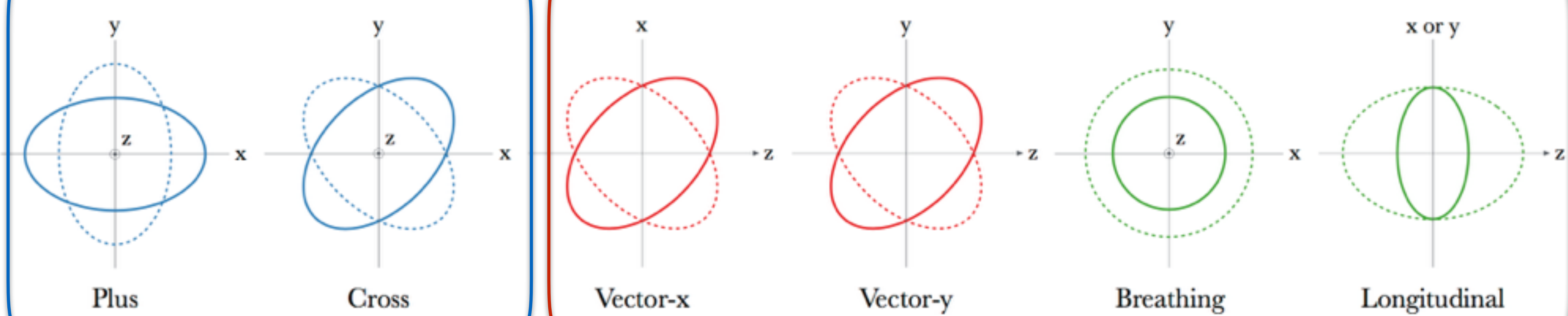

Predicted by GR

Modification of GR

Callister et al, Phys.Rev. X7 (2017) no.4, 041058

BACKGROUND FROM DIFFERENT POLARIZATIONS

Assume background from different polarizations is uncorrelated

$$\Omega_{\rm GW}(f) = \Omega^T(f) + \Omega^V(f) + \Omega^S(f)$$

$$\gamma(f) \propto \sum_A \int e^{2\pi i f \hat{\mathbf{\Omega}}\cdot\Delta\mathbf{x}/c} F_1^A(\hat{\mathbf{\Omega}}) F_2^A(\hat{\mathbf{\Omega}}) d\mathbf{\Omega},$$

antenna patterns

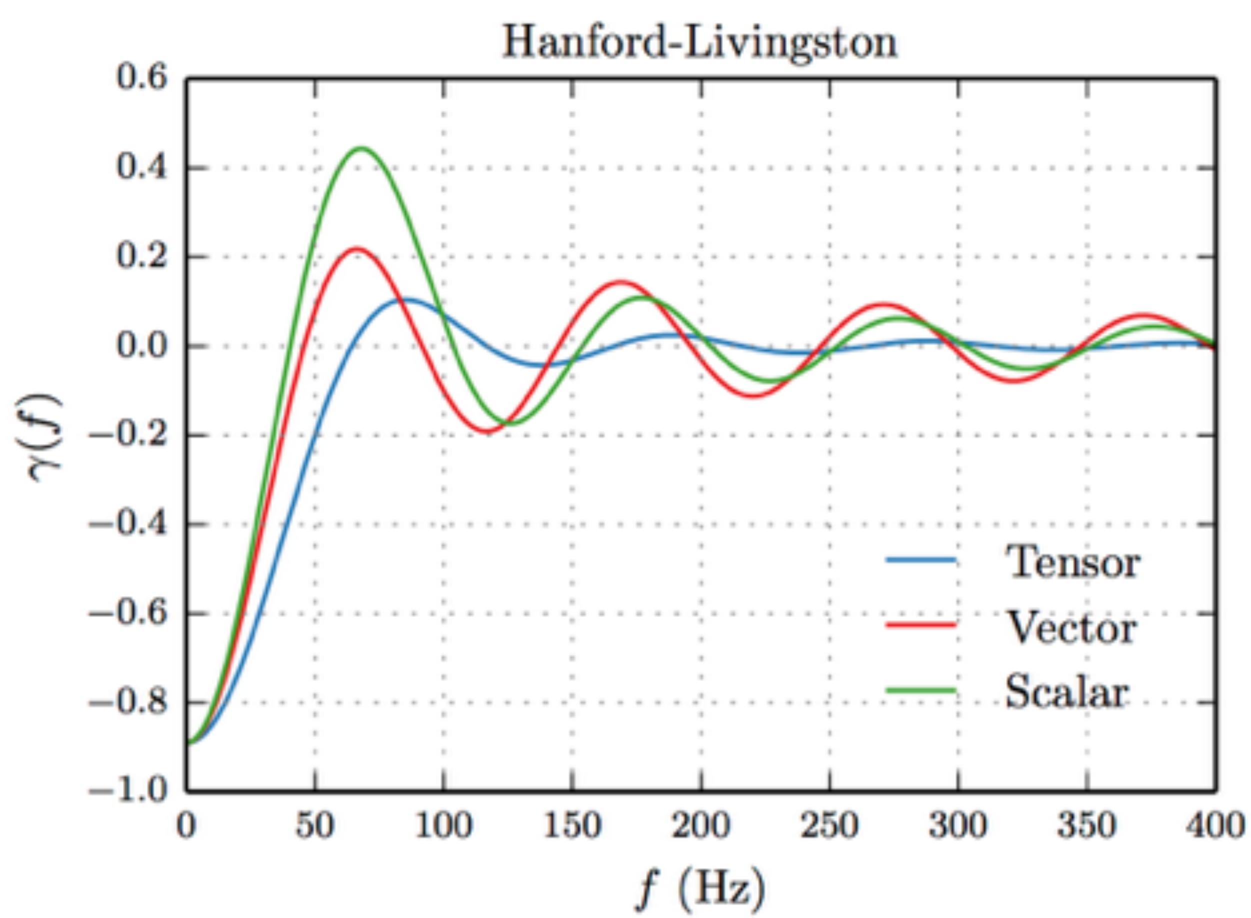

Callister et al, Phys.Rev. X7 (2017) no.4, 041058

ILLUSTRATION OF BASIC IDEA

Very loud injection

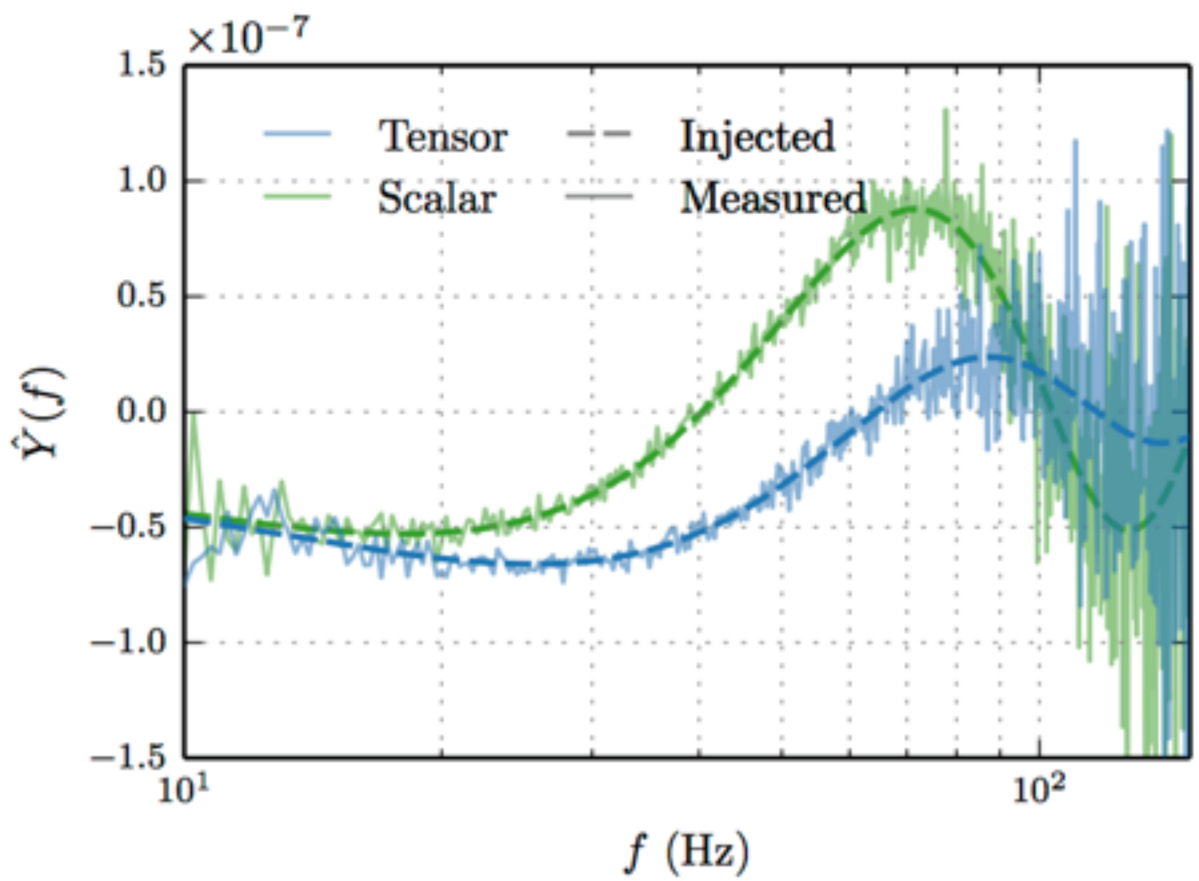

More ‘realistic’ injection

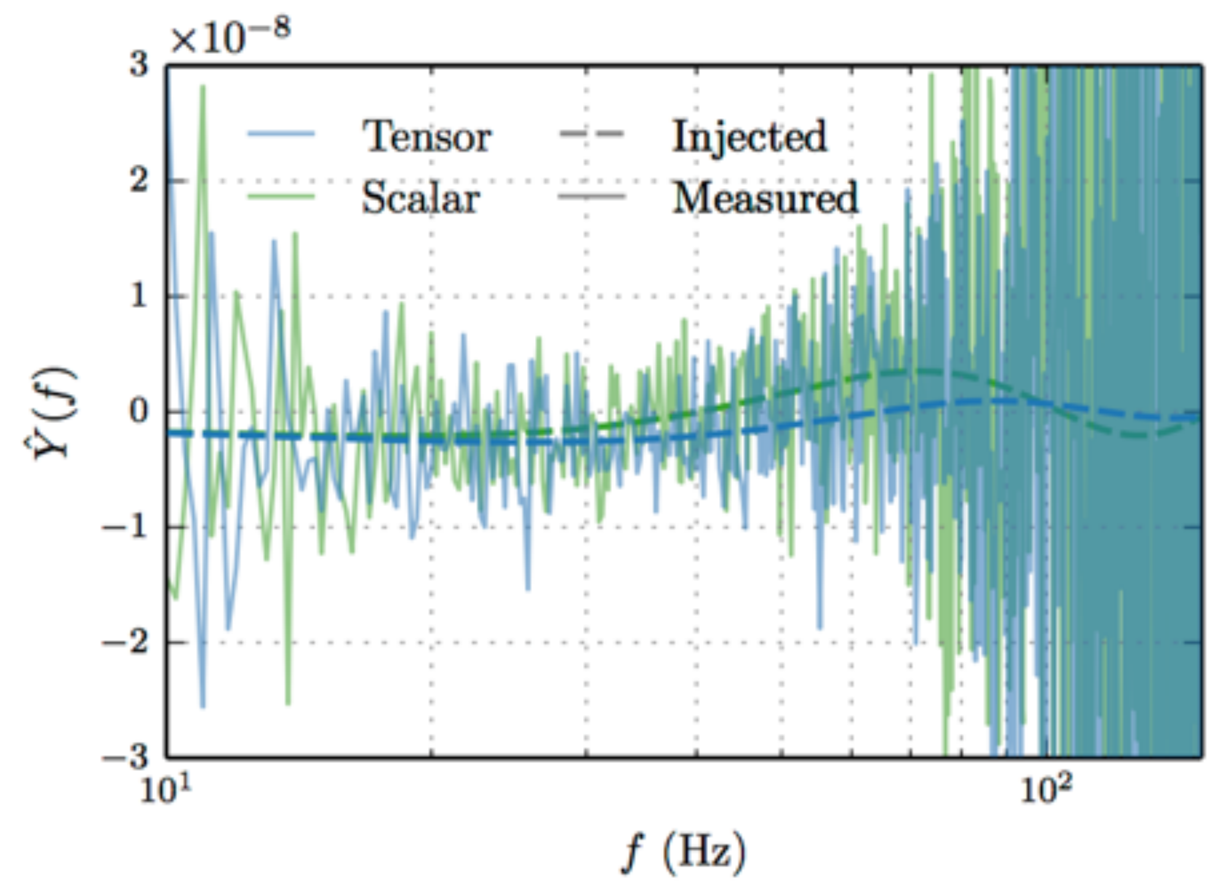

Can use differences in the overlap reduction functions to separate different polarizations

Callister et al, Phys.Rev. X7 (2017) no.4, 041058

DISTINGUISHING VECTOR AND SCALAR: WHERE A NETWORK HELPS

Recovery applied to injection of Scalar+Tensor background

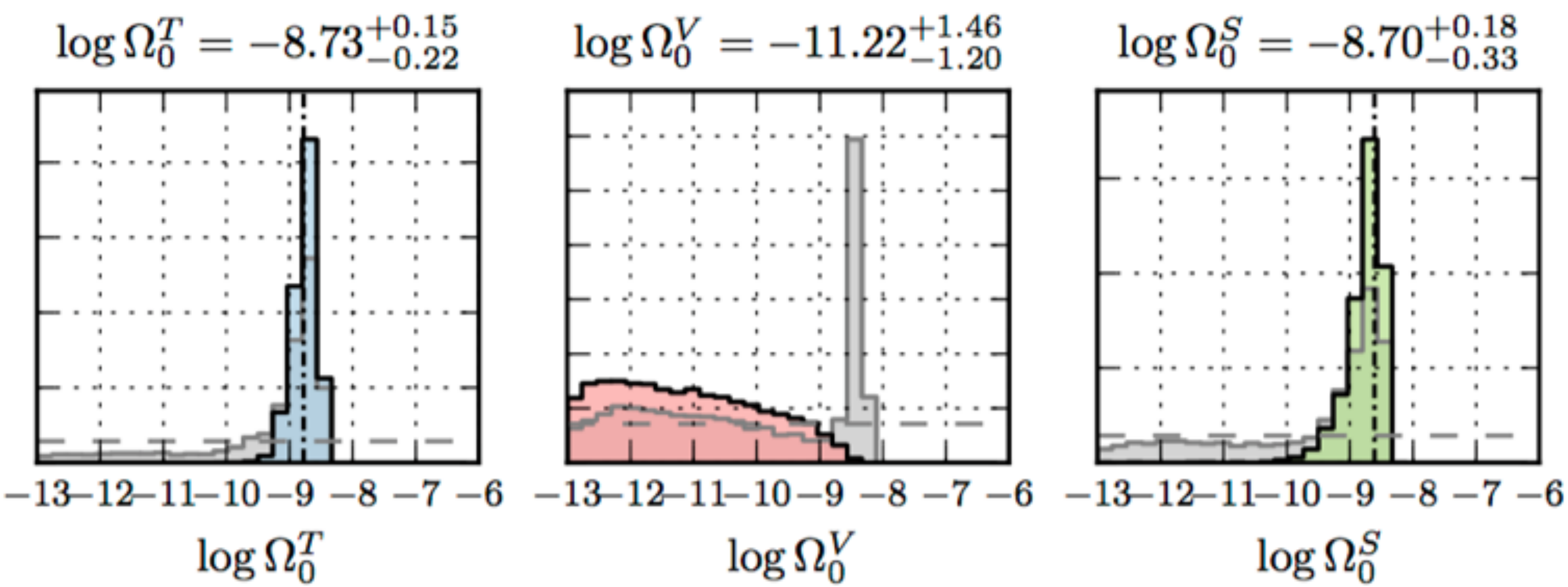

Grey: PE with Advanced LIGO only (likes both V and S)

Color: PE with Advanced LIGO+Virgo (correctly prefers S only)

Additional detectors can help distinguish polarizations

Callister et al, Phys.Rev. X7 (2017) no.4, 041058

01 SEARCH RESULTS (HL ONLY, NO NETWORK)

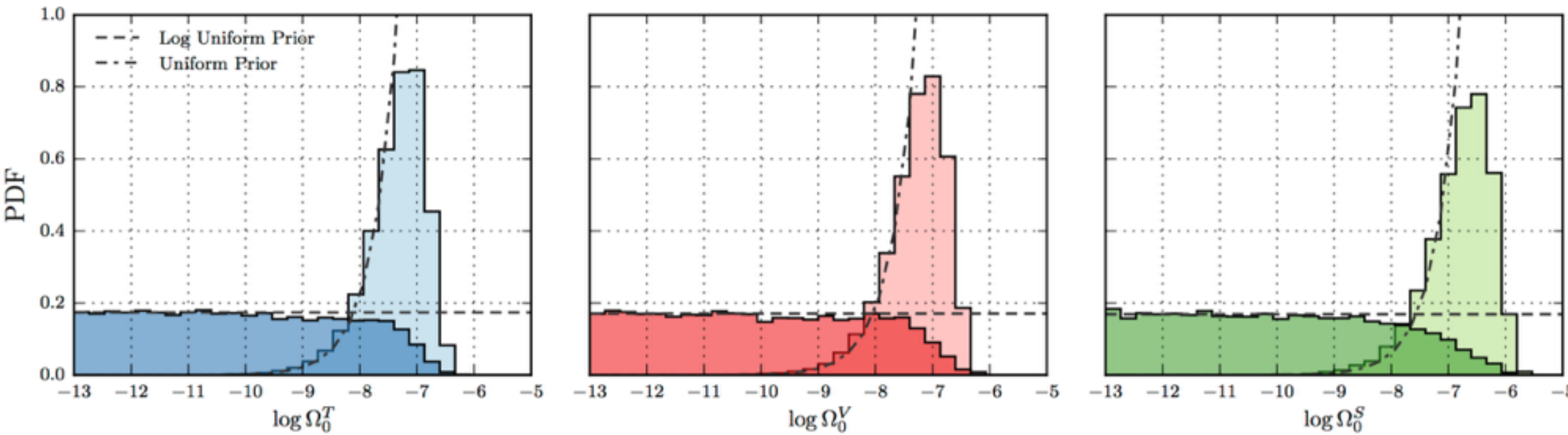

Prior	log Ω_0^T	log Ω_0^V	log Ω_0^S	Ω_0^T	Ω_0^V	Ω_0^S
Log-Uniform	−7.25	−7.20	−6.96	5.6×10^{-8}	6.4×10^{-8}	1.1×10^{-7}
Uniform	−6.70	−6.59	−6.07	2.0×10^{-7}	2.5×10^{-7}	8.4×10^{-7}

Abbott et al, Phys.Rev.Lett. 120 (2018) no.20, 201102

SUMMARY

- Stochastic background is a target for future detection
- Astrophysical background may be in reach by advanced detectors
- A detector network can help by
  - Improving sensitivity
  - Improving localization
  - Improving polarization measurements